Available online at www.sciencedirect.com

SciVerse ScienceDirect

Ceramics International 39 (2013) 1821–1826

CERAMICS INTERNATIONAL

www.elsevier.com/locate/ceramint

In situ fabrication mechanism of a dense Sr and Ca doped lanthanum chromite interconnect on Ni-YSZ anode of a solid oxide fuel cell during co-sintering

A. Heidarpour[a,*], A. Saidi[a], M.H. Abbasi[a], G.M. Choi[b]

[a]Department of Materials Engineering, Isfahan University of Technology (IUT), Isfahan 84156-83111, Iran
[b]Fuel Cell Research Center and Department of Materials Science and Engineering, Pohang University of Science and Technology, Pohang 790-784, Republic of Korea

Received 10 June 2012; received in revised form 4 July 2012; accepted 10 August 2012
Available online 18 August 2012

Abstract

In this study fabrication mechanism of a dense Sr and Ca doped lanthanum chromite interconnect on Ni-YSZ anode of a solid oxide fuel cell after co-sintering is investigated. Based on the understanding of sintering mechanism, a dense $La_{1-x-y}Sr_xCa_yCrO_{3-\delta}$ interconnect membrane was successfully prepared on the anode support of NiO-YSZ by a novel method. In this method a base layer of $La_{0.8}Sr_{0.2}CrO_{3-\delta}$ was screen printed on NiO-YSZ substrate and a top layer of $CaCrO_4$ was then coated and co-sintered at 1400 °C. $CaCrO_4$ not only melts and fills the open pores in the base layer, but it also dissolves in it forming La_{1-x-y} $Sr_xCa_yCrO_{3-\delta}$ as a single layer. The mechanism of $CaCrO_4$ dissolution in the base layer, densification characteristics and microstructure of interconnect are discussed.

Keywords: A. Sintering; Densification mechanism; Doped lanthanum chromite ceramics; Interconnect

1. Introduction

The interconnector of solid oxide fuel cells (SOFC) not only provides the conductive path for electrical current to pass from the anode of one cell to the cathode of the next one, but it is also required to separate the fuel gas from the oxidant. So, it should be dense, sufficiently conductive, and stable in both oxidizing and reducing atmospheres [1]. Because of these tough requirements, only few materials can be used for SOFC interconnector. Lanthanum chromite ($LaCrO_3$) materials satisfy many of the requirements [2]; thus, they have been extensively investigated [3–5]. This part of SOFC still remains to be a main challenge holding back single fuel cells from being compiled into stacks [1,2]. Considering that lanthanum chromite interconnector is hard to be co-sintered with green anode, resulting in a high cost for manufacturing, some investigators fabricated interconnector rather than $LaCrO_3$ [6]. To the best of our knowledge, there are few reports on dense doped lanthanum chromite ceramic interconnect membrane on porous anode support by the potentially cost-effective co-firing process. Wang et al. fabricated a dense $La_{0.7}Ca_{0.3}CrO_3$ interconnect thin membrane on NiO/$Sm_{0.2}Ce_{0.8}O_{2-\delta}$/$La_{0.7}Ca_{0.3}Cr_{0.97}O_{3-\delta}$ anode substrates by co-firing [7]. In a previous study [8], we prepared a dense single layer of $La_{1-x-y}Sr_xCa_yCrO_{3-\delta}$ by a novel bilayer $CaCrO_4$/$La_{0.8}Sr_{0.2}CrO_{3-\delta}$ interconnector via co-sintering with green NiO-YSZ anode. In this method a base layer of $La_{0.8}Sr_{0.2}CrO_{3-\delta}$ was screen printed on NiO-YSZ substrate and a top layer of $CaCrO_4$ was then coated and co-sintered at 1400 °C. It was found that during sintering, not only $CaCrO_4$ melts and fills the open pores in the base layer, but it also dissolves in that forming $La_{1-x-y}Sr_xCa_yCrO_{3-\delta}$ as a single layer. The $La_{1-x-y}Sr_xCa_yCrO_{3-\delta}$ composition has been studied by some investigators for SOFC interconnect material due to its good electrical conductivity and stability during cooling and heating cycles [9]. In Ca-doped lanthanum

*Corresponding author. Tel.: +98 0311 3915762; fax: +98 0311 3912751.
E-mail address: a.heidarpour@gmail.com (A. Heidarpour).

0272-8842/$ - see front matter © 2012 Elsevier Ltd and Techna Group S.r.l. All rights reserved.
http://dx.doi.org/10.1016/j.ceramint.2012.08.029

chromite (LCC) some $CaCrO_4$ existed as second phase which exsoluted from perovskite due to poor alkaline earth solubility below 1200 °C and during sintering the $CaCrO_4$ was melted and enhanced densification [10–12]. In this work, the mechanism of $CaCrO_4$ dissolution in $La_{0.8}Sr_{0.2}CrO_3$ layer, based on the mechanism of sintering of lanthanum chromite doped with Ca or Sr is investigated.

2. Experimental procedure

$La_{0.8}Sr_{0.2}CrO_3$ (LSC20) and $CaCrO_4$ (CC) specimens were prepared by the glycine nitrate process (GNP) [13] which has been explained elsewhere [8]. For homogenization, the synthesized powder was milled with zirconia balls (10 and 5 mm diameter) at 100 rpm in ethyl alcohol for 6 h. To remove any organic residuals, the powders were then calcined at 500 °C for 30 min. NiO powder (99.97%, Kojundo Chemical, Japan) and YSZ powder (TZ-8YS, 99.9%, Tosoh, Japan) were used as the starting materials to synthesize NiO-YSZ composite as anode. Ten weight percent of corn starch was added as a pore former for the anode substrates. NiO and YSZ with the weight ratio of 6:4 were milled for 18 h in ethanol and dried subsequently. The composite powders were then die-pressed (25 mm diameter) and pre-sintered at 950 °C for 1 h. The screen printing paste was made by mixing the powder with alpha-terpineol, ethyl cellulose and ethylene glycol. All pastes were 3-roll milled (EXAKT 50, Exakt, Germany) for uniform powder distribution. In order to fabricate an interconnect thin membrane, a base layer of $La_{0.8}Sr_{0.2}CrO_{3-\delta}$ was screen printed on NiO-YSZ substrate and a top layer of $CaCrO_4$ was then coated and co-sintered at 1400 °C for 10 h to form $La_{1-x-y}Sr_xCa_yCrO_{3-\delta}$ as a single layer. The screen-printing process with mesh size screen thickness was used to change the thickness of the laminate prior to sintering. The thickness of base layer (LSC20) was kept constant at 30 μm while two thicknesses of 30 and 50 μm were used for the top layer of $CaCrO_4$. These two samples were named as LSC20/CC30 and LSC20/CC50, respectively. Phase determination in the samples was carried out by a XRD-Rigaku diffractometer using Cu K_α radiation ($\lambda = 1.5406$ Å). Microstructures of the sintered bodies and interconnect membranes were observed using a field emission scanning electron microscope JEOL-JSM-6330F equipped with EDS microanalyzer. DTA analysis of the samples were carried out at a heating rate of 10 °C/min in a temperature range between 700 and 1200 °C using SQT-Q600.The ohmic resistance and area specific resistance (ASR) were measured at 800 °C in dual atmosphere [8]. The electrical measurement was performed after reduction of NiO in anode for 5 h in 97% H_2+3% H_2O gas at 800 °C. Area specific resistance (ASR) was measured by impedance spectra. The obtained resistance was interconnector resistance because anode contains Ni in its composition and its resistance is negligible.

3. Results and discussion

3.1. Doped lanthanum chromite membrane preparation

Fig. 1 shows the SEM micrographs of co-sintered interconnector and anode for two composite layers as LSC20/CC30 and LSC20/CC50 after sintering at 1400 °C for 10 h. In addition the two-layer system is shown in Fig. 1a. Both composite layers were dense and as seen the interconnector layer with initial 30 μm CC top layer (LSC20/CC30) is about 10 μm and quite dense despite the presence of a few closed pores. In the case of 50 μm CC top layer (LSC20/CC50), some liquid sank down to the bottom and mixed with substrate which was undesirable.

Fig. 2 shows the XRD patterns of final membrane surface of the two LSC20/CC30 and LSC20/CC50 composite layers. The interconnect made of LSC20/CC30 composite layers showed pure rhombohedral perovskite structure, indicating no other phase whilst the interconnect

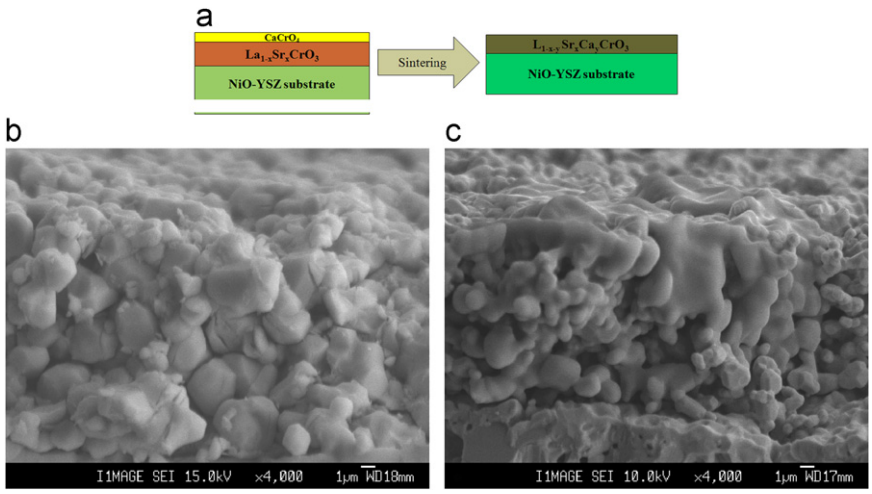

Fig. 1. (a) Schematic representation of bilayer interconnect and anode before and after sintering, (b) and (c) cross-section SEM micrographs of LSC20/CC30 and LSC20/CC50 samples, respectively.

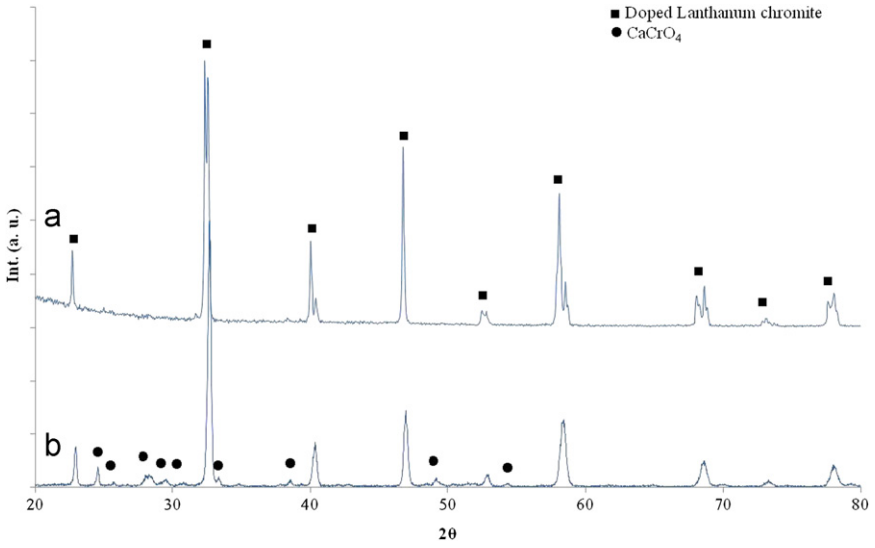

Fig. 2. XRD pattern of (a) LSC20/CC30 and (b) LSC20/CC50 interconnects after sintering at 1400 °C for 10 h.

made of LSC20/CC50 composite layers showed orthorhombic perovskite structure as well as some $CaCrO_4$ as a second phase. Actually in LSC20/CC50 composite layer the amount of $CaCrO_4$ was high and undesirable. So, no further investigation was carried out on this sample. As a sintering mechanism for doped lanthanum chromite, it can be suggested that liquid phase forming species like $CaCrO_4$ help sintering and densification. This species melt and dissolve in lanthanum chromite during sintering. If the amount is low, it disappears and no second phase can be detected [14]. The area specific resistance (ASR) between anode and interconnector at 800 °C was measured in dual atmosphere [8] and LSC20/CC30 and for LSC20/CC50 samples were 0.0089 and 10 $\Omega\,cm^2$, respectively.

Ruka and Kuo [15] fabricated a dense doped lanthanum chromite interconnect thin membrane on an electrode by two step co-sintering. They used a two layer technique which consisted of using doped lanthanum chromite as base layer and a top layer such as $CaO+Al_2O_3$ or $SrO+Al_2O_3$ and co-sintering at 1550 °C. Although they made a dense layer of doped lanthanum chromite but the sintering temperature was too high to be suitable for co-sintering of different parts of solid oxide fuel cells. In addition, they did not report the resistance between interconnect and electrode.

3.2. Densification mechanism

As mentioned above, during heating to sintering temperature, $CaCrO_4$ melts at 1100 °C and gradually fills the open pores in the base layer of LSC20 ($La_{0.8}Sr_{0.2}CrO_3$). The liquid phase formation was confirmed by the DTA test (Fig. 3). As shown, the onset of melting takes place at nearly 1100 °C and the curve displays a single step melting process. The liquid phase surrounding the LSC20 particles is shown schematically in Fig. 4. It has been reported [10] that the liquid phase shows good wetting and spreading characteristics which is desirable for optimum liquid phase sintering.

It is known that $CaCrO_4$ loses oxygen (Fig. 3) and forms a solid solution with $LaCrO_3$ [10]. The dissolution reaction can be written as:

$$xCaCrO_4+(1-x)\,LaCrO_3 \rightarrow La_{1-x}Ca_xCrO_3+x/2O_2 \quad (1)$$

This reaction will proceed with the diffusion of calcium and chromium ions from liquid phase into the perovskite phase of LSC20 during subsequent heating at high temperatures. The dissolution reaction of $CaCrO_4$ into LSC20 ($La_{0.8}Sr_{0.2}CrO_3$) can be written similar to Eq. (1) as below:

$$xCaCrO_{4(l)}+(1-x)\,La_{0.8}Sr_{0.2}CrO_{3(s)} \rightarrow La_{0.8-0.8x}Sr_{0.2-0.2x}Ca_xCrO_{3(s)}+x/2O_{2(g)} \quad (2)$$

This process of dissolution consequently induces a change in the composition of the liquid phase. As a result, the Ca/Cr ratio increases in liquid phase and a more Ca rich liquid will form. The divergent behavior of the $CaCrO_4$ composition and densification may be understood by referring to the $CaO–Cr_2O_3$ phase diagram after the work of Kaiser et al. [16]. The change in composition of $CaCrO_4$, while heating depends on the kinetics of dissolution of $CaCrO_4$ into lanthanum chromite. As heating continues, the liquid composition changes toward CaO and solid β-$CaCr_2O_4$ disappears leading to the formation of a complete liquid phase.

Differential thermal analysis also indicated a deviating behavior. Referring to Fig. 3, $CaCrO_4$ should produce a DTA curve with two melting peaks, one near 1022 °C, the eutectic temperature, and the other at a higher temperature upon complete melting of the liquid. Conversely, the DTA curve, contains only one broad peak, beginning at 1078 °C.

Actually the reaction occurs at the interface between LSC20 grains and liquid phase, increasing the calcium content in LSC20 in the vicinity of interface. As the

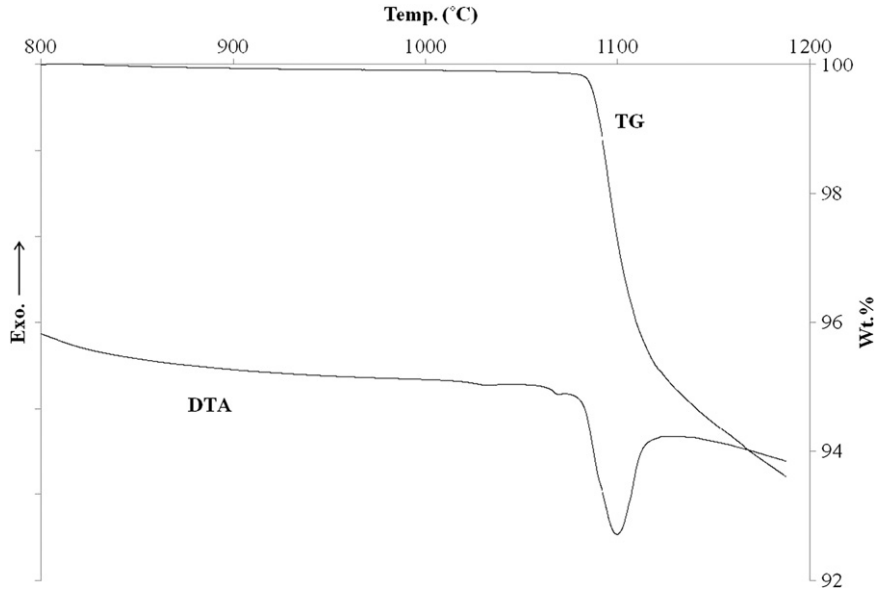

Fig. 3. TG-DTA curve for the melting of $CaCrO_4$.

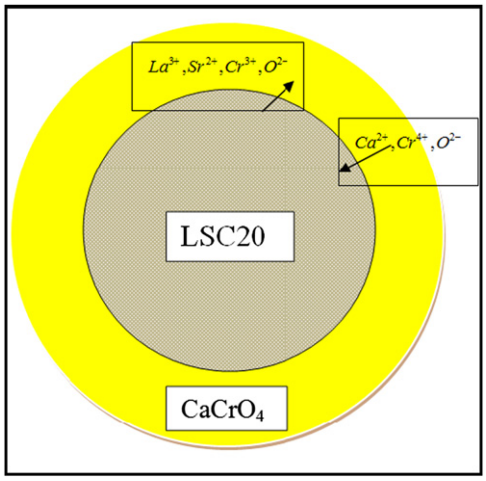

Fig. 4. A schematic representation of $CaCrO_4$ liquid surrounding the LSC20 particle.

temperature is increased, the Ca solubility also increases and Ca, Cr and O dissolve in the perovskite matrix.

By the reaction between LSC20 grains and liquid phase, Ca and Cr ions and liberated oxygen can move easily through the liquid phase at grain boundaries and the rapid grain growth and pore elemination may occur, which are characteristics of a liquid phase assisted sintering mechanism. The diffusion coefficients of different species are high enough either in grain boundray or bulk [17] to ensure homogenization after 10 h sintering at 1400 °C. It is confirmed by Fig. 2, where XRD pattern of LSC20/CC30 interconnect after sintering at 1400 °C for 10 h shows pure rhombohedral perovskite structure, indicating no other phase.

Fig. 5 shows the XRD pattern for reaction products at the surface of anode after removing interconnect layer for the LSC20/CC30 bilayer sample. No diffraction peaks of secondary phases were detected for LSC20/CC30 sample and only peaks of NiO and YSZ were identified. So for the interconnect made of LSC20/CC30 bilayer sample, the amount of liquid phase has been enough leading to no second phase formation. In addition, LSC20 powder was prepared by glycine nitrate process (GNP) and had a high specific surface ($22\ m^2\ g^{-1}$). This high surface area of the base layer causes high surface contact between liquid phase and LSC20 grains and the kinetics of dissolution is enhanced. In contrast, XRD pattern of the interconnect layer made of LSC20/CC50 bilayer sample shows $CaCrO_4$ other than perovskite structure in the diffraction pattern (Fig. 2b) because of high thickness of $CaCrO_4$ top layer. Fig. 6 shows the XRD pattern for reaction products at the surface of anode after removing interconnect layer for the LSC20/CC50 bilayer sample. As seen, some $CaZrO_3$ and $CaCr_2O_4$ as secondary phases are observed at the surface of anode in contact with interconnect layer. In fact, in LSC20/CC50 bilayer sample some $CaCrO_4$ melt reached the anode surface and reacted with YSZ as reported by Carter et.al. [18].

4. Conclusions

The main results obtained from this research work can be concluded as follows:

1. Densification mechanism for co-sintering of doped lanthanum chromite interconnects on Ni-YSZ anode substrate for SOFC application was investigated. Two layers of $La_{1-x}Sr_xCrO_{3-\delta}$ and $CaCrO_4$ (as top layer) were applied on NiO-YSZ substrate and then co-sintered. So, a dense $La_{1-x}Sr_xCa_yCrO_3$ layer was fabricated.

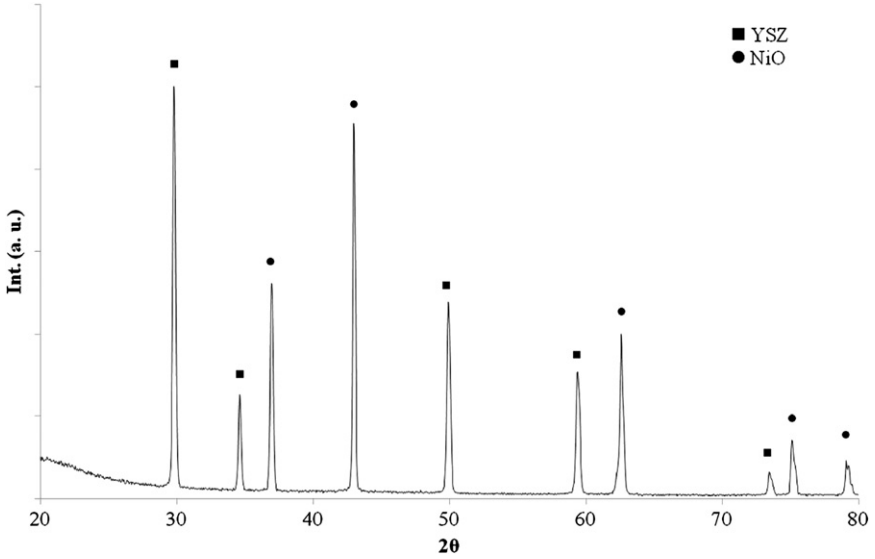

Fig. 5. XRD pattern of the anode surface after removing interconnect layer for LSC20/CC30 sample.

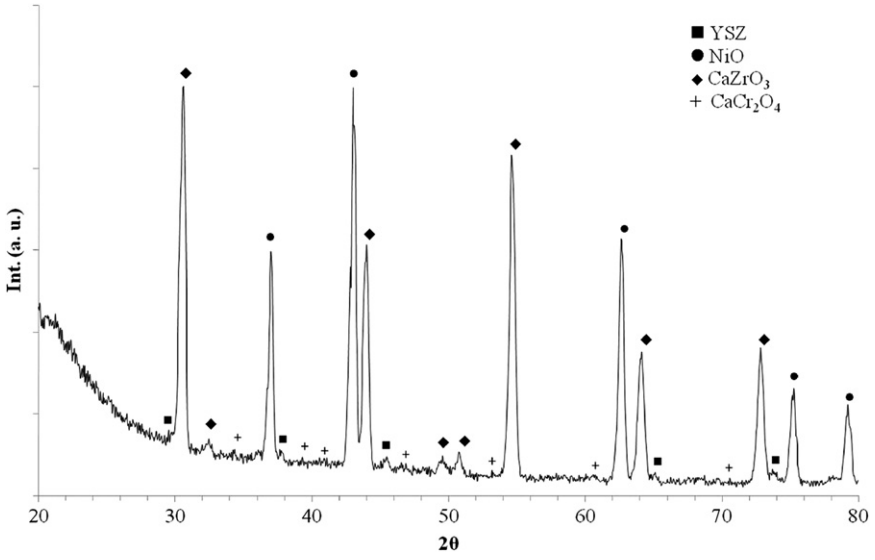

Fig. 6. XRD pattern of the anode surface after removing interconnect layer for LSC20/CC50 sample.

2. LSC20/CC30 bilayer combined well together where the same thickness was used and sintered at 1400 °C for 10 h.
3. $CaCrO_4$ not only melts during sintering and fills the open pores in the base layer, but it also dissolves in the base layer. The liquid phase surrounds the base layer grains and the dissolution reaction between LSC20 grains and liquid phase occurs. Ca and Cr ions and liberated oxygen can move easily through the liquid phase at grain boundaries and the rapid grain growth and pore elimination occur, which are characteristics of a liquid phase assisted sintering mechanism.
4. Interconnect made of LSC20/CC30 bilayer sample, after sintering at 1400 °C for 10 h had pure rhombohedral perovskite structure. In this case, almost all $CaCrO_4$ phase dissolved in LSC20 base layer and no second phase was detected at anode surface, indicating that the amount of liquid phase was enough.

References

[1] N.Q. Minh, T. Takahashi, Science and Technology of Ceramic Fuel Cells, Elsevier, New York, 1995.
[2] J.W. Fergus, Lanthanum chromite-based materials for solid oxide fuel cell interconnects, Solid State Ionics 171 (2004) 1–15.
[3] B. Lin, S. Wang, X. Liu, G. Meng, Simple solid oxide fuel cells, Journal of Alloys and Compounds 490 (1–2) (2010) 214–222.
[4] L.F.G. Setz, S.R.H. Mello-Castanho, R. Moreno, M.T. Colomer, Physicochemical characterization of strontium- and cobalt-doped lanthanum chromite powders produced by combustion synthesis, International Journal of Ceramics Technology 6 (5) (2009) 625–635.

[5] Y.P. Fu, H.C. Wang, S.H. Hu, K.W. Tay, Electrical conduction behaviors of isovalent and acceptor dopants on B site of $(La_{0.8}Ca_{0.2})CrO_{3-\delta}$ perovskites, Ceramics International 37 (7) (2011) 2127–2134.
[6] Y. Xu, S. Wang, R. Liu, T. Wen, Z. Wen, A novel bilayered $Sr_{0.6}La_{0.4}TiO_3/La_{0.8}Sr_{0.2}MnO_3$ interconnector for anode-supported tubular solid oxide fuel cell via slurry-brushing and co-sintering process, Journal of Power Sources 196 (2011) 1338–1341.
[7] S. Wang, Y. Dong, B. Lin, J. Gao, X. Liu, G. Meng, Fabrication of dense $LaCrO_3$ based interconnect thin membrane on anode substrates by co-firing, Materials Research Bulletin 44 (2009) 2127–2133.
[8] A. Heidarpour, G.M. Choi, M.H. Abbasi, A. Saidi, A novel approach to co-sintering of doped lanthanum chromite interconnect on Ni-YSZ anode substrate for SOFC applications, Journal of Alloys and Compounds 512 (2012) 156–159.
[9] A. Mitsui, K. Homma, Y. Kumekawa, F. Nakamura, N. Ohba, Y. Hoshino, T. Hashimoto, Preparation of $La_{1-x-y}Ca_xSr_yCrO_3$ with high-density structural phase transition and electrical conduction properties, Journal of the Electrochemical Society 155 (5) (2008) A395–A403.
[10] J.D. Carter, M.M. Nasrallah, H.U. Anderson, Liquid phase behavior in nonstoichiometric lanthanum chromites, Journal of Materials Science 31 (1996) 157–163.
[11] S. Wang, B. Lin, Y. Chen, X. Liu, G. Meng, Evaluation of simple, easily sintered $La_{0.7}Ca_{0.3}Cr_{0.97}$ $O_{3-\delta}$ perovskite oxide as novel interconnect material for solid oxide fuel cells, Journal of Alloys and Compounds 479 (2009) 764–768.
[12] N. Sakai, T. Kawada, H. Yokokawa, M. Dokiya, I. Kojima, Liquid-phase-assisted sintering of calcium-doped lanthanum chromites, Journal of the American Ceramic Society 76 (3) (1993) 609–616.
[13] L.A. Chick, L.R. Pederson, G.D. Maupin, J.L. Bates, L.E. Thomas, G.J. Exarhos, Glycine nitrate combustion synthesis of oxide ceramic powders, Materials Letters 10 (1990) 6–12.
[14] L.A. Chick, J. Liu, J.W. Stevenson, T.R. Armstrong, D.E. McCready, G.D. Maupin, G.W. Coffey, C.A. Coyle, Phase transitions and transient liquid-phase sintering in calcium-substituted lanthanum chromite, Journal of the American Ceramic Society 80 (8) (1997) 2109–2120.
[15] R.J. Ruka, L.J.H. Kuo, Electrode and Method of Interconnection Sintering on an Electrochemical Cell, US Patent no. 5277995, 1994.
[16] A. Kaiser, B. Sommer, E. Woermann, The system $CaO–CaCr_2O_4–CaAl_2O_4$ in air and under mildly reducing conditions, Journal of the American Ceramic Society 75 (1992) 1463–1471.
[17] T. Horita, M. Ishikawa, K. Yamaji, N. Sakai, H. Yokokawa, Masayuki Dokiya, Cation diffusion in $(La,Ca)CrO_3$ perovskite by SIMS, Solid State Ionics 108 (1998) 383–390.
[18] J.D. Carter, C.C. Appel, M. Mogensen, Reactions at the calcium doped lanthanum chromite-yttria stabilized zirconia interface, Journal of Solid State Chemistry 122 (1996) 407–415.